ACS Sustainable Chemistry & Engineering

Research Article

pubs.acs.org/journal/ascecg

Wood-Derived Carbons with Hierarchical Porous Structures and Monolithic Shapes Prepared by Biological-Template and Self-Assembly Strategies

Liaoyuan Xia,*[,†,‡] Xianjun Li,[†] Yiqiang Wu,*[,†] and Minzhi Rong[‡]

[†]College of Material Science and Engineering, Central South University of Forestry and Technology, Changsha 410004, P. R. China

[‡]Materials Science Institute, Sun Yat-Sen University, Guangzhou 510275, P. R. China

Supporting Information

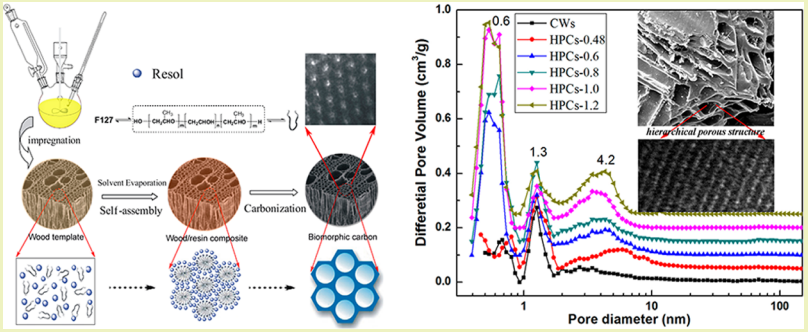

ABSTRACT: Novel wood-derived hierarchical porous carbons (HPCs) with biomimicry macro-/microporous and ordered mesostructures have been successfully prepared by using wood processing residues, such as poplar powder/or shavings, as a mimic-template to reproduce the wood cellular structures, resol as a precursor, and triblock copolymer F127 as a soft-template to construct the mesostructure onto the wood scaffold. X-ray diffraction, scanning electron microscopy, transmission electron microscopy, and N_2 adsorption results indicate that the obtained HPCs not only faithfully reproduce the wood cellular structures but also possess ordered mesostructures (p6 mm) with uniform pore sizes (~4.0 nm) and high surface areas (~463m^2/g). Furthermore, the pore texture and properties of HPCs could be regulated by simply varying the dosages of resol precursor to poplar shavings. A formation process for wood-derived HPCs with controlled hierarchical nanostructures through wood-template and interface self-assembly approaches is proposed in this work. In addition, HPCs exhibit good adsorption properties toward organic vapors, demonstrating that this kind of HPCs could be used as a promising material for adsorbents and separation systems.

KEYWORDS: *Biomimetic, Dual-template, Ordered mseostructure, Hierarchically porous structure, Carbonaceous materials*

INTRODUCTION

Hierarchical porous carbons (HPCs), as a novel type of nanostructured materials, have received considerable interest as candidates for electrochemical capacitors, lithium ion batteries, solar cells, hydrogen storage systems, sorbent for toxic gas separation, and so on due to their well-defined pore dimensions and topologies.[1−9] Compared to conventional porous carbonaceous materials, HPCs could improve the diffusibility of guest species through its unique hierarchical pores and more open framework.[1] As we know, macropores could minimize diffusive resistance to mass transport, while the micro/mesopores could provide high surface areas and large pore volumes that will benefit active sites dispersion. Therefore, much effort has been focused on the design and construction of hierarchically structured materials with desired nanoscaled pores and topologies, such as HPCs or the monolithic materials with hierarchically porous structures.[9,10] Up to now, fabrication of well-defined HPCs has been mainly carried out using various template-assisted methods, such as hard-/soft-templating approaches, dual-template routes, or templating and post-activation combination methods, etc.[11−17] However, each of these methods has limitations, such as most of the soft-/hard templates are chemical products, high-cost and nonrenewable. In particular, the post-activation approach or hard-template method requires additional processing steps that are usually time-consuming, and a collapse of the regular nanostructure would easily occur during the removal of templates.

Recently, biological-templates have been demonstrated to be a green and efficient way to construct hierarchical porous materials.[18−26] This is because materials from nature can be renewable and environmental friendly, especially those that are morphologically complex with sophisticated structures and

Received: March 26, 2015
Revised: June 24, 2015
Published: July 1, 2015

DOI: 10.1021/acssuschemeng.5b00243
ACS Sustainable Chem. Eng. 2015, 3, 1724−1731

Scheme 1. Scheme for Fabrication of HPCs with Ordered Mesostructures by Wood-Template and Self-Assembly Methods

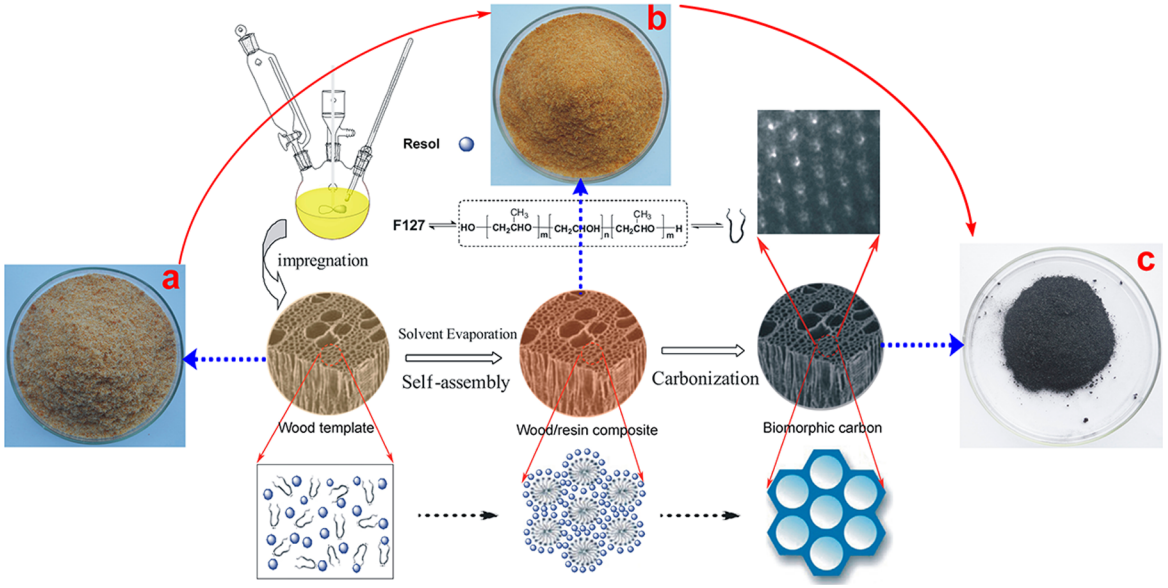

ordering, which can be adjustable over a wide range of length scales. It is well known that wood is not only environmental friendly and renewable but also has complex hierarchically porous structures and open cellular cavities, such as the micrometer scale of the cell diameter and wall, and the nanometer level of the molecular fiber and membrane. More importantly, the open cellular cavities and hierarchical pores are easily accessible by the impregnation method via liquid or gaseous infiltration. Therefore, these features make wood a perfect template candidate for generating porous materials with both structural and morphological complexity and especially suitable to be directly converted into activated carbons or monolithic inorganic materials.[27−30]

Nevertheless, although the macro-/microporosity can be easily created by reproduction of these natural systems and potassium hydroxide activation, there exists a difficulty in the formation of ordered mesostructures for the wood-derived porous materials, thus limiting its application in the fields of selective catalysis, adsorption, or separation, etc. Specifically, the chemical activation procedures often involve rigid reaction conditions and potassium hydroxide, which is not in accordance with the urgent requirements of low-cost and environmental protection. Obviously, the above drawback would be completely overcome if the ordered mesostructure could be incorporated into wood cellular structures by a simple self-assembly method. As we all know, the solvent-evaporation-induced self-assembly is a sol−gel process which relates with a liquid-deposition coating technique to fabricate 2D materials, such as thin films and monoliths during solvent evaporation.[31,32] Therefore, a controllable evaporation-induced coating and self-assembly on a decomposable 3D scaffold, such as polymer- or/and biological-template scaffold would be a desirable strategy for preparation of hierarchically porous monoliths.[10] To date, although great progress has been made in the biological-template route to fabricate hierarchical porous materials, to the best of our knowledge, it remains a great challenge to develop a simple but efficient route to achieve faithful reproduction of the wood cellular structures while endowing the hierarchical porous materials with ordered mesostructures.

Herein, for the first time, we developed a facile strategy for preparation of a novel type of HPCs with biomimicry macro-/micropores and ordered mesostructures by using poplar shavings as a mimetic template to reproduce the cellular structures, with resol as a precursor and triblock copolymer F127 as a soft-template to assemble mesostructures onto the surface of wood cellular structures. The fabrication procedure mainly involves four steps as shown in Scheme 1; the evaporation-induced coating and interface self-assembly method could explain the formation process for the ordered mesostructures of HPCs.

EXPERIMENTAL SECTION

Chemicals. All chemicals were used as received without further purification. Poly(ethylene oxide)-*b*-poly(propylene oxide)-*b*-poly(ethylene oxide) triblock copolymer Pluronic F127 ($EO_{106}PO_{70}EO_{106}$, M_W = 12600) was bought from Aldrich. Phenol, formalin solution (37%), sodium hydroxide, and ethanol were obtained from Sinopharm Chemical Reagent Company. Deionized water was used in all the experiments. Commercial activated carbon YP-50F was purchased from the Kuraray Group. Poplar shavings were chosen as the biological templates and extracted by ethanol for 6 h at 60 °C and then dried at 80 °C for 24 h under vacuum.

Preparation of Phenol−Formaldehyde (PF) Resin Precursor. In a typical procedure, 6.1 g of phenol was completely melted at 42 °C in a flask; then, 1.3 g NaOH solution (20 wt %) was slowly added with stirring over a period of 15 min. After that, 10.5 g formalin (37 wt %) was added, and the mixture was heated at 70−72 °C for 1 h. After cooling to room temperature, the pH was adjusted to 7.0 by using a 2.0 M HCl solution. Water was then removed under vacuum below 50 °C. The final product (M_w < 500) was dissolved in ethanol (40 wt %).

Preparation of HPCs. In a typical synthetic procedure, 10 g of F127 was dissolved in 70 g of ethanol and stirred at 40 °C for 1 h to obtain a clear solution. Then, 50 g of the resol solution mentioned above was slowly added, and the mixture was further stirred for 1.5 h. The solution was prepared according to the mass ratios of resol/F127/ethanol = 2:1:10.

DOI: 10.1021/acssuschemeng.5b00243
ACS Sustainable Chem. Eng. 2015, 3, 1724−1731

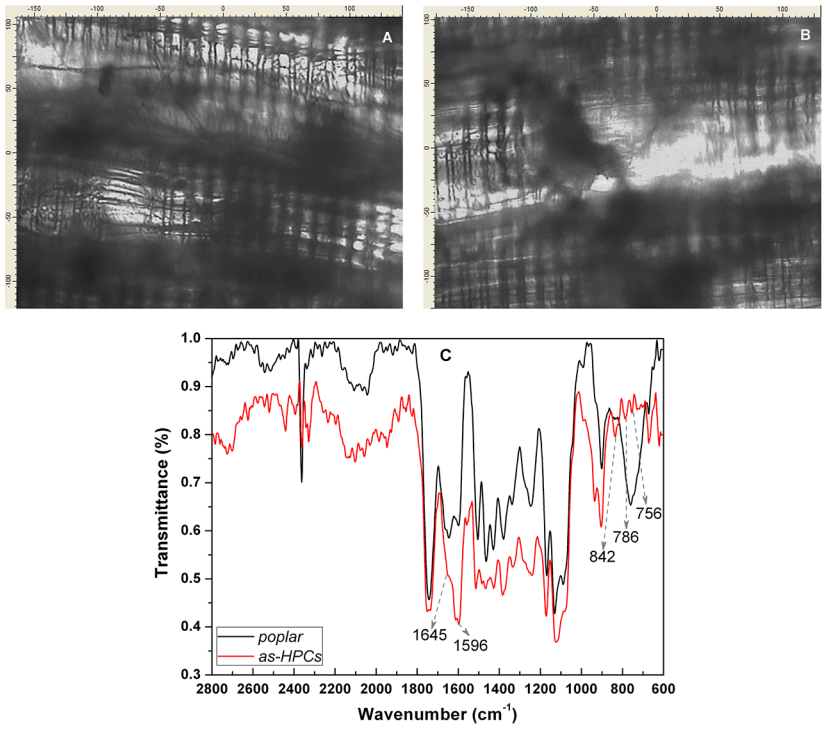

Figure 1. FTIR microspectroscopy (C) of poplar shavings and as-made HPCs with corresponding micrographs: (A) poplar shavings and (B) as-made HPCs.

After that, the obtained homogeneous solution was infused into 20 g of treated poplar shavings under pressure and then slowly stirred over 60 min until the poplar shavings are fully saturated with the above precursor solution. Then, the completely impregnated poplar shavings were cast onto open dishes, followed by evaporation of the solvent for 24 h at 40 °C, and further thermosetted at 105 °C for 24 h. The obtained samples were denoted as as-HPCs-*x*, wherein *x* represents the mass ratio of PF to poplar shavings. Last, the as-made samples were placed in an alumina boat and pyrolyzed at 900 °C for 3 h under an argon atmosphere in a tubular furnace. The heating rate was 3 °C/min below 600 and 5 °C/min above 600 °C. The hierarchically biomorphic carbons were obtained and were denoted as HPCs-*x*-*y*, wherein *x* represents the mass ratio of PF to poplar shavings and *y* represents the temperature of pyrolysis. The original poplar shavings directly carbonized product was denoted as CWs. Moreover, it is worth noting that this strategy also provides a new way to prepare hierarchically porous carbonaceous monoliths by additionally molding the as-made HPCs and then pyrolyzing at high temperature, as shown in Figure S1 of the Supporting Information. A typical process is as follows: 105 g of the sample of as-HPCs was poured into a metalline mold and then compressed into plate shape with dimensions of 100 mm (length) × 100 mm (width) × 10 mm (height) under a pressure of 0.8 MPa for 15 min at 150 °C. After that, the plate-like sample was pyrolyzed at the same experimental conditions as mentioned above; monolithic HPCs were obtained.

Characterization. Powder X-ray diffraction (XRD) patterns were conducted on a Rigaku 2200 diffractometer using a Cu Kα radiation source (40 kV, 30 mA) with a 2θ range from 0.6° to 5°. All of the samples were scanned under the same conditions. Transmission electron microscopy (TEM) images were obtained on a HITACHI H-800 microscope operated at 200 kV. Scanning electron microscopy (SEM) was conducted using a Quantan 450 at 15 kV. An N_2 adsorption measurement was carried out using a Micromeritics ASAP 2020 analyzer at 77 K. Before the measurements, all samples were degassed at 250 °C under vacuum for 5 h. The BET surface area (S_{BET}) was analyzed by the Brunauer−Emmett−Teller (BET) theory. The external surface area (S_{ext}) and micropore surface area (S_{mic}) was determined by the *t*-plot theory. The pore size distribution was analyzed by the original density functional theory (DFT) combined with non-negative regularization and medium smoothing. The adsorption properties toward organic vapors were studied with a Hiden IG-3 intelligent gravimetric analyzer. Thermogravimetric analysis (TGA) was performed on a Netzsch TG-209 instrument at a heating rate of 10 °C/min under a nitrogen atmosphere. Fourier-transform infrared (FTIR) microspectroscopy was conducted using a Bruker EQUINOX 55 FT-IR spectrometer.

RESULTS AND DISCUSSION

Formation of Hierarchical Porous Structures. As illustrated in Scheme 1, a simple and feasible dual-template strategy for fabrication of wood-derived HPCs is described in detail. First, a homogeneous solution of resol precursor and triblock copolymer F127 in ethanol was prepared. Then, the above solution was continuously poured into poplar shavings by the impregnation method under pressure. After a period of infiltration, the resol precursor was gradually coated onto the cellular walls and channels of the poplar shavings. This is due to the strong hydrogen bonding interaction between the resol and the surface of the poplar cellular walls. With a further increase in concentration (c > CMC, the critical micelle concentration), the resol precursor assembled with the F127 triblock copolymer to form ordered mesostructured resol polymers on the interface of the poplar cellular walls.[10,33] The thickness of the polymer depends on the mass ratio of the resol precursor to poplar

DOI: 10.1021/acssuschemeng.5b00243
ACS Sustainable Chem. Eng. 2015, 3, 1724−1731

shavings. After the ethanol completely evaporated, the poplar shavings still kept its original shape and size (Figure S1, Supporting Information, as-made HPCs). This implied that the resol precursor was infused into cellular structures of the poplar shavings, which could be confirmed by FTIR microspectroscopy. As shown in Figure 1A and B, the appearance of the original poplar shavings and as-made HPCs is remarkably similar, both exits tube-like cells structure, which is consistent with SEM observations (Figure 2A,B). Nevertheless, the

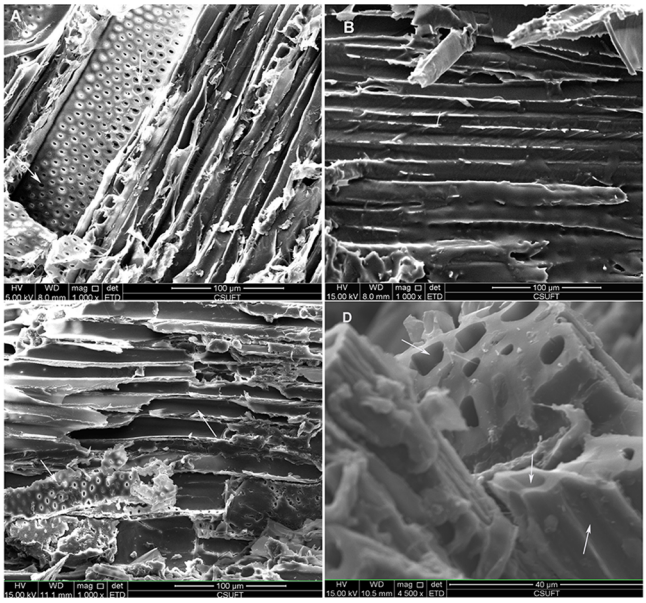

Figure 2. SEM micrographs of (A) cellular structure of the original poplar shavings, (B) as-HPCs-0.8, (C) HPCs-0.8-700 (parallel to the vessels direction), and (D) HPCs-0.8-700 (sectional areas of the vessels).

corresponding FTIR spectra provide more information (Figure 1C). For the as-HPCs-0.8, it can be seen that the characteristic peak at 1596 cm^{-1} is attributed to skeletal stretching vibration for lignin in wood. Although the characteristic band of the phenylene peak might overlap the lignin peak at around 1600 cm^{-1}, the appearance of the shoulder at 1645 cm^{-1} still reflects the existence of phenyl groups, and the peaks around at 756, 784, and 842 cm^{-1} also reflect the existence C−H bending vibrations for the phenyl groups. It is further confirmed that the resol precursors have been successfully coated onto the surface of the cellular walls, which is in good accordance with the SEM analysis. In addition, the peak around 2400 cm^{-1} is attributed to the background information on CO_2. Lastly, the pyrolysis process was carried out by slowly increasing temperature from 40 to 350 °C to achieve a uniform shrinkage and avoid a collapse of the nanostructure regularity. After further carbonization at a higher temperature (350−900 °C), the F127 templates can be removed about 380 °C (Figure 6), while the phenolic resin and poplar shavings directly converted into carbons during the carbonization process. As a result, the ordered mesoporous carbon yielded on the interface of the poplar struts, and wood-derived HPCs can be obtained.

To further understand fabrication of the wood-derived HPCs, the morphologies of the original poplar shavings, as-made HPCs, and the wood-derived HPCs were investigated using the SEM technique. As shown in Figure 2A, many opening pits (marked with arrow) exist on the cellular walls and membrane of poplar shavings, which act as channels to connect different tracheidal cells, so that it is easy for the precursor solution to infiltrate into the cellular structures. The surface of the cellular walls become smooth (Figure 2B) after the impregnation process, implying that the cellular walls have been successfully coated by resol precursors during solvent evaporation, which is in well accordance with FTIR microspectroscopy results (Figure 1). Figure 2C and D (marked with arrows) and Figure S4 of the Supporting Information show that the resulting HPCs still keep the same external and internal morphology as the original wood cellular structures after pyrolyzed at high temperature (700 °C, 900 °C). Besides, the photograph in Figure S3A and B of the Supporting Information also demonstrates that the as-HPCs-1.0 almost kept its external shape and size. But the colors changed from thin yellow to dark brown due to the partial oxidization of phenol during the process of thermopolymerization.

Moreover, an important feature of the monolithic HPCs is its stable and regulable bulk form. It can be found that the monolithic HPCs-1.0-700 retains its plate-like shape with obvious shrinkage after carbonization processing (Figure S3, Supporting Information), although its color turns from dark brown to black because of carbonization. The calculating data indicate that the shrinkage is about 27% in linear dimensions and 43% in volume, and the carbonization yield is about 29%. By further grinding the monolithic HPCs-1.0-700, we can obtain a powdery sample of HPCs-1.0-700 (Figure S3ESupporting Information).

Mesostructure Analysis. Figure 3 and Figure S2 of the Supporting Information display XRD profiles of HPCs after

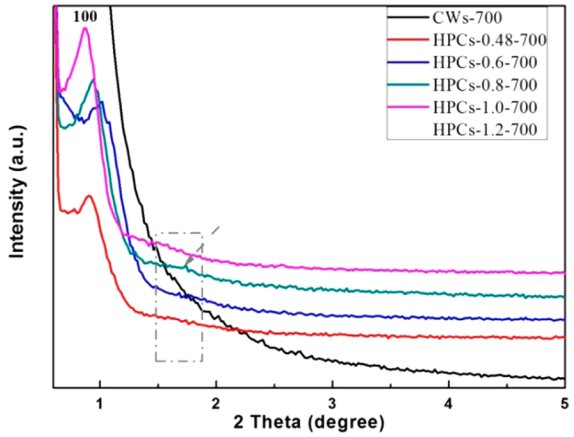

Figure 3. XRD patterns of HPCs with different PF/poplar shaving mass ratios after pyrolyzed in argon at 700 °C.

carbonization at high temperature under argon atmospheres. It is clearly shown that no peaks can be found in the low-angle region of CWs, indicating that no ordered mesostructures exist, and TEM observation sustains this opinion (Figure 4A, inset). Compared to the CWs, the XRD patterns of all HPCs show a resolved diffraction peak, which can be indexed as [100] reflections of a 2D hexagonal mesostructure. The structural assignments based on the XRD patterns can be demonstrated by TEM images (Figure 4B−F). More interestingly, with a rise in PF/W mass ratios, narrower and more intense diffraction peaks are presented at low-angle regions, which suggests the ordered mesostructures of HPCs is enhanced accordingly. After further carbonization at 900 °C, the characteristics of the XRD

DOI: 10.1021/acssuschemeng.5b00243
ACS Sustainable Chem. Eng. 2015, 3, 1724−1731

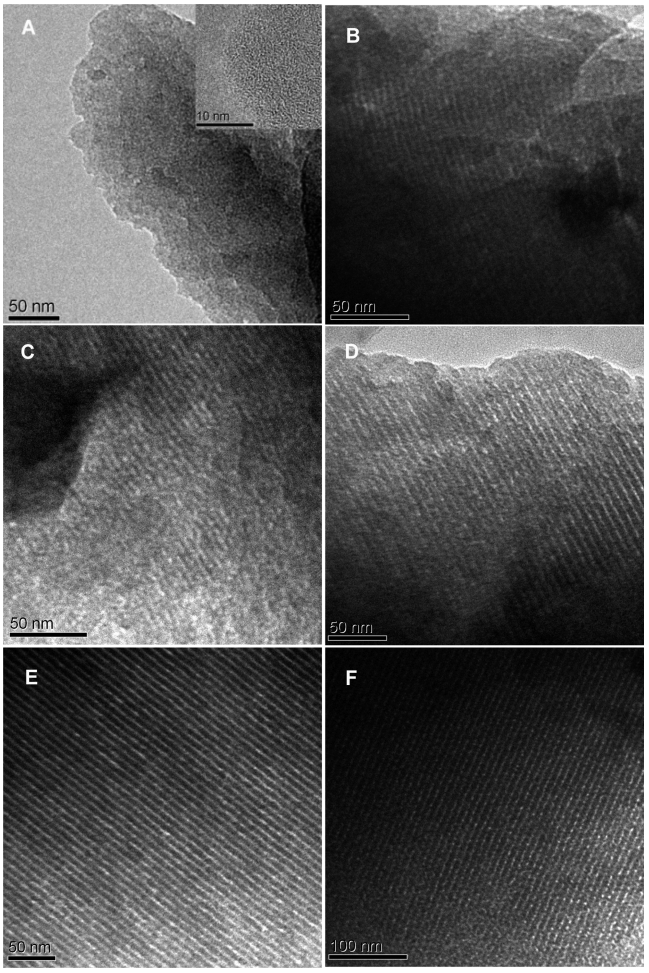

Figure 4. TEM images of HPCs with different PF/wood shaving mass ratios: (a) CWs, (B) HPCs-0.48-700, (C) HPCs-0.6-700, (D) HPCs-0.8-700, (E) HPCs-1.0-700, and (F) HPCs-1.2-700 viewed along the [100] and [001] directions.

pattern of HPCs can also be observed (Figure S2, Supporting Information), indicating that the ordered mesostructure is thermally stable. Nevertheless, sharp diffraction peaks are observed at higher angles, owing to the mesostructural further shrinkage at higher temperature.

To reveal more refined structural features, TEM investigations were performed for HPCs with different PF/W mass ratios. As shown in Figure 4A, the CWs display a disordered worm-like nanoporous appearance, which mainly results from wood tissues through high temperature carbonization. As the mass ratios of PF/W increase to 0.48, however, pronounced changes in the TEM images with weakly striped-like mesostructures were observed (Figure 4B). When the mass ratios were further increased to 0.8, HPCs displayed large domains of striped-like and hexagonally arrayed patterns viewed along the [110] and [001] directions, respectively (Figure 4D–F). Clearly, the above TEM observation of HPCs show that the PF/W mass ratios are closely related to the mesostructures of HPCs, which is in good accordance with the XRD analysis. This is due to the ordered mesostructure strongly depending on the PF assemble with the F127 to form an ordered mesophase resol polymer onto the surface of the wood cellular walls, and the thickness of the polymer is directly related with the mass ratio of the resol precursor to poplar shavings. To further probe the component of the samples, we used an energy-dispersive X-ray (EDX) measurement to analyze the CWs and HPCs. As displayed in Figure S5 of the Supporting Information, the EDX spectrum on the randomly selected area only showed the existence of the C element.

N_2 Sorption Characteristics. The N_2 adsorption method is used to further quantitatively elucidate the hierarchical porous structure of HPCs. As shown in Figure 5a, all the isotherms are a combination of types I and IV, and the step rise of the initial part of the isotherm evidences the presence of plentiful micropores. It is shown that the CWs exhibit an atypical type IV isotherm with an obvious H3 hysteresis loop, and the adsorption and desorption branches are apparently not close at low relative pressure, indicating the presence of partly interstitial nanopores. However, HPCs show typical type IV curves with mass ratios of PF/W increasing from 0.48 to 1.2, and the hysteresis loops are more like H4 type, which corresponds to limited amounts of mesopores limited by micropores. It is also further confirmed that the mesostructure of HPCs can be adjusted by the mass ratios of PF/W, which is consistent with the above XRD and TEM results. Moreover, the adsorption amount increases gradually and does not reach a

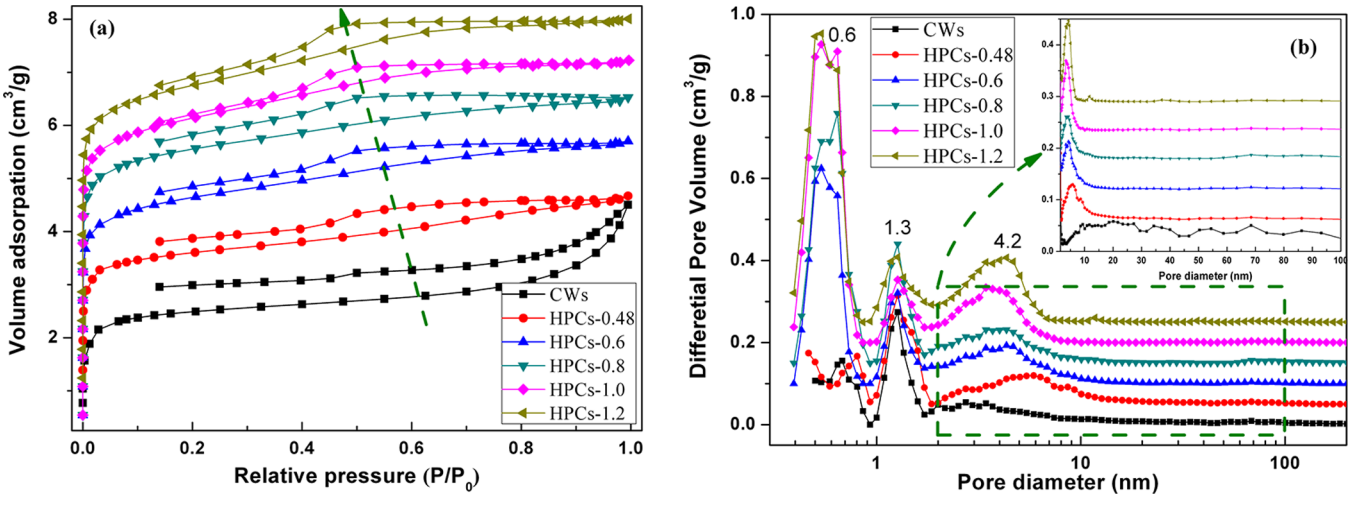

Figure 5. (a) N2 adsorption–desorption isotherm of HPCs and corresponding (b) DFT pore size distribution.

DOI: 10.1021/acssuschemeng.5b00243
ACS Sustainable Chem. Eng. 2015, 3, 1724–1731

Table 1. Synthetic Conditions and Structural Parameters of All Samples Pyrolyzed at 700°C[a]

samples	(PF/W) (g/g)	S_{BET} (m^2/g)	S_{mic} (m^2/g)	S_{ext} (m^2/g)	V_T (cm^3/g)	D_p (nm)	yield (wt %)
CWs	0	151.6	97.4	54.3	0.119	7.3	20.7
HPCs-0.48	0.48	209.3	140.4	68.9	0.132	4.0	26.5
HPCs-0.6	0.6	351.5	244.6	106.8	0.198	3.3	27.5
HPCs-0.8	0.8	418.7	310.9	107.7	0.226	3.2	28.1
HPCs-1.0	1.0	463.8	330.9	132.9	0.251	3.0	28.7
HPCs-1.2	1.2	459.6	324.3	135.3	0.253	3.1	29.8
YP-50F	–	1600	–	–	0.70	–	–

[a]Notes: PF/W is the mass ratio of phenol–formaldehyde resin to poplar shavings. S_{BET}, S_{ext}, S_{mic}, V_t, and D_p are the BET surface area, external surface area, micropore surface area, total pore volume, and BJH adsorption average pore diameter, respectively. Yield = (quality of HPCs/quality of PF and wood) × 100%. YP-50F is commercial activated carbon.

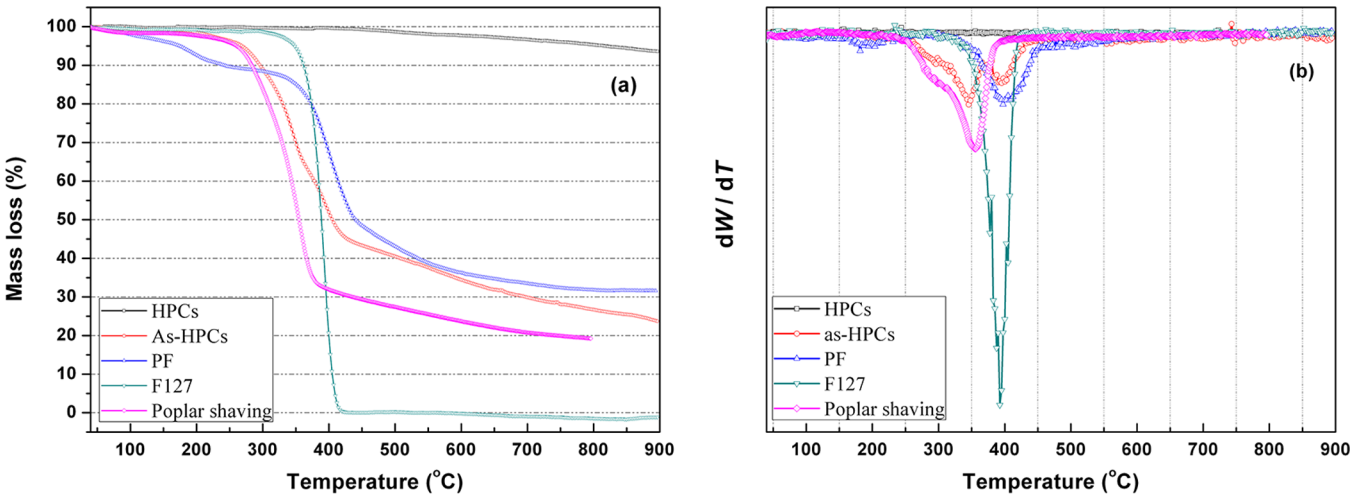

Figure 6. TGA (a) and corresponding DTG (b) curves of the original poplar shavings, copolymer surface F127, PF resins, and as-made and HPCs-1.0-700 under nitrogen atmosphere.

plateau near the P/P_0 of 1.0, also demonstrating the presence of mesopores and macropores.[18]

The pore size distribution (PSD) curves obtained using density functional theory (DFT) are displayed in Figure 5b; three obvious regions can be confirmed. For all HPCs, bimodal PSD peaks at 0.6 and 1.3 nm could be observed, which are mainly ascribed to slot-shape pore and networks formed by PF resin polymer and/or wood fiber through pyrolysis. Furthermore, all HPCs displayed a narrow mesoporous PSD peak at ~4.0 nm (Figure 5b, inset) except for the CWs, which result from the resol precursor assembled with the F127 triblock copolymer. The result is well in accordance with both the XRD analysis and TEM observations. Interestingly, the first PSD peak and the mesoporous PSD peak are closely correlated with the mass ratios of PF/W. As the mass ratios of PF/W increase, their peak intensity gradually enhances. It should be noted that the macropores formed from the micrometer-scaled cell channels and walls are not reflected in the PSD curves but verified by SEM observation (Figure 2C and D), which is probably due to capillary condensation. Furthermore, data describing the pore texture of the mesostructured HPCs based on nitrogen-sorption experiments are listed in Table 1. It is clear that the BET surface areas, micropore surface areas, external surface areas, total pore volume, and carbonization yield of HPCs also showed a growth trend with the mass ratios of PF/W increasing from 0 to 1.2 (Table 1). By simply adjusting the mass ratios of PF/W, the mesostructure of HPCs is gradually changed to an ordered 2-D hexagonal structure, and the surface areas and pore volumes are increasing accordingly.

Thermogravimetric Analysis. It is clearly shown in Figure 6a that the TGA curves of the original poplar shavings display notable weight losses at about 352 °C, which correspond to the observed weight loss of ~79% below 700 °C. Similarly, the TGA curve of the PF resin displays about 1.9% of a weight loss from 100 to 200 °C, which may be related to the polymerization of the phenolic resins. The subsequent weight loss (~36%) between 400 to 800 °C can be mostly attributed to decomposition of the PF resins. This implies that the poplar shavings and PF resin have a generally trend to thermal decomposition during the carbonization process. Furthermore, it should be noted that the TGA curve of the copolymer template F127 under a N_2 atmosphere shows a weight loss of about 100 wt % at 410 °C, suggesting that the triblock copolymer template can be removed by carbonization above 410 °C in N_2. Thus, the TGA curve of as-HPCs-1.0 shows a weight loss (~9 wt %) at about 280 °C, which corresponds to partial decomposition of the poplar (Figure 6). The subsequent weight loss (~45%) between 350 to 410 °C can be mostly attributed to F127 entirely removed. Further weight loss of 22 wt % in the range of 410–900 °C is detected, which may be related to the polymerization of phenolic resins and further decomposition of the poplar.

The corresponding DTG curve (Figure 6b) also confirms that the temperature range of decomposition of as-HPCs-1.0 is coincident with the wood template and PF precursors. A significant weight loss (~55 wt %) in the range of 300–500 °C is observed, which is mainly attributed to the decomposition of the wood template (350 °C), triblock copolymer F127

DOI: 10.1021/acssuschemeng.5b00243
ACS Sustainable Chem. Eng. 2015, 3, 1724–1731

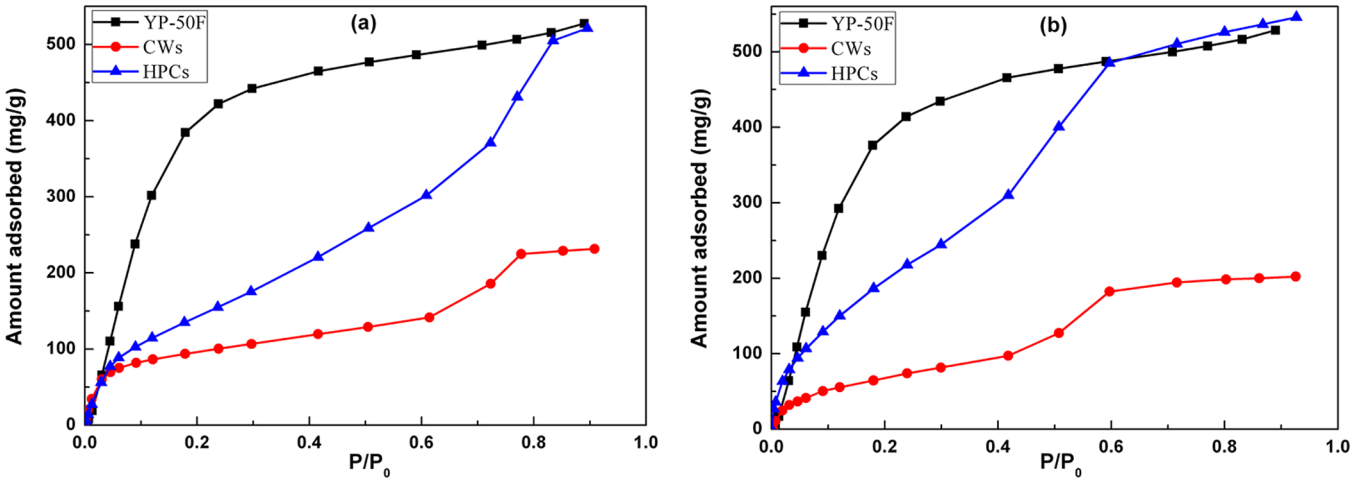

Figure 7. Adsorption isotherms of methanol vapor (a) and benzene vapor (b) for YP-50F, CWs, and HPCs-1.0-700.

template (392 °C), and PF resins (398 °C). In addition, the TGA curve for the wood-derived HPCs only shows a weight loss of about 6.6 wt % above 700 °C (Figure 6a), suggesting that HPCs have goodl thermal stability.

Adsorption Property. To demonstrate the adsorption ability of the wood-derived HPCs with ordered mesostructures, the adsorption behaviors toward organic vapors were studied by contrast with CWs and commercially activated carbon YP-50F. It is clearly shown that the wood-derived HPCs had a superior adsorption performance toward organic vapors such as methanol and benzene at various relative pressures than the poplar shavings directly carbonized product, denoted as CWs. This is mostly owing to the BET surface area difference between HPCs and CWs that could play a key role in the adsorption properties (463 vs 151m^2/g). The adsorption behavior of porous carbon materials toward organic vapors not only is directly related to BET surface area, pore size distribution, and porous structures, but also has a close relationship to the relative pressure and surface chemical groups. Usually, the adsorption capacity continuously increases with the relative pressure because the organic vapors in mesopores and macropores will continue to condensation. Therefore, we found that HPCs had a similar adsorption performance toward organic vapors at high relative pressures as YP-50F (Figure 7), although HPCs had a smaller BET surface area than YP-50F (463 vs 1600m^2/g). This indicated that HPCs have more efficient pore surface utilization, which is most likely due to the positive synergistic effect of their unique hierarchically micro/macroporous and ordered mesostructures,[18] but activated carbon YP-50F only has a microporous structure. Moreover, it should be noted that the pore surface chemistry difference between HPCs and YP-50F could play a role in the adsorption property. That is to say, it was demonstrated that HPCs could be used as good candidates for adsorbents and separation systems.

CONCLUSIONS

In summary, we have successfully for the first time prepared a novel type of HPCs that have mimicry cell structures, ordered mesostructures (p6 mm) with uniform pore sizes (~4.0 nm), and high surface areas (~463m^2/g). By simply varying the mass ratio of the resin precursor to poplar shavings, the pore texture and properties of HPCs could be regulated. The wood-derived HPCs exhibit good adsorption properties toward organic vapors, demonstrating that this kind of HPCs could be used as a promising material for adsorbents and separation systems. More importantly, this strategy provides a new avenue for effective combination of the biological-template and self-assembly methods to prepare HPCs with controlled hierarchically porous structures and monolithic shapes. In this way, wood processing residues can also be sustainably utilized for extra value.

ASSOCIATED CONTENT

Supporting Information

Figures S1−S5, including schematic drawing, XRD patterns, photographs, and SEM and EDX spectra. The Supporting Information is available free of charge on the ACS Publications website at DOI: 10.1021/acssuschemeng.5b00243.

AUTHOR INFORMATION

Corresponding Authors

*E-mail: xly1516@126.com. Phone/fax: +86-20-84114008.
*E-mail: wuyq0506@126.com. Phone/fax: +86-20-84114008.

Notes

The authors declare no competing financial interest.

ACKNOWLEDGMENTS

This work was supported by the National Forestry Industry Research Special Funds for Public Welfare Projects (Grant 201204708), NSF of China (Grants 31200438, 31370564), Doctoral Program Foundation of Institutions of Higher Education of China (Grant 20124321120002), and Hunan Provincial Natural Science Foundation of China (Grants 2015JJ2199). We greatly thank graduate L. C. Tian and Mr. W. H. Chen for experimental and characterization assistance.

REFERENCES

(1) Zou, C.; Wu, D. C.; Li, M. Z.; Zeng, Q. C.; Xu, F.; Huang, Z. Y.; Fu, R. W. Template-free fabrication of hierarchical porous carbon by constructing carbonyl crosslinking bridges between polystyrene chains. *J. Mater. Chem.* **2010**, *20*, 731.

(2) Zeng, Q. C.; Wu, D. C.; Zou, C.; Xu, F.; Fu, R. W.; Li, Z. H.; Liang, Y.; Su, D. S. Template-free fabrication of hierarchical porous carbon based on intra-/inter-sphere crosslinking of monodisperse styrene−divinylbenzene copolymer nanospheres. *Chem. Commun.* **2010**, *46*, 5927.

DOI: 10.1021/acssuschemeng.5b00243
ACS Sustainable Chem. Eng. 2015, 3, 1724−1731

(3) Qie, L.; Chen, W. M.; Xu, H. H.; Xiong, X. Q.; Jiang, Y.; Zou, F.; et al. Huang. Synthesis of functionalized 3D hierarchical porous carbon for high-performance supercapacitors. *Energy Environ. Sci.* **2013**, *6*, 2497−2504.
(4) He, X. J.; Zhao, N.; Qiu, J. S.; Xiao, N.; Yu, M. X.; Yu, C.; et al. Synthesis of hierarchical porous carbons for supercapacitors from coal tar pitch with nano-Fe2O3 as template and activation agent coupled with KOH activation. *J. Mater. Chem. A* **2013**, *1*, 9440−9448.
(5) Wang, J. C.; Oschatz, M.; Biemelt, T.; Borchardt, L.; Senkovska, I.; Lohe, M. R.; Kaskel, S. Synthesis, characterization, and hydrogen storage capacities of hierarchical porous carbide derived carbon monolith. *J. Mater. Chem.* **2012**, *22*, 23893.
(6) Parlett, C. M. A.; Wilson, K.; Lee, A. F. Hierarchical porous materials: catalytic applications. *Chem. Soc. Rev.* **2013**, *42*, 3876.
(7) Song, C.; Du, J.; Zhao, J. H.; Feng, S. A.; Du, G. X.; Zhu, Z. P. Hierarchical Porous Core−Shell Carbon Nanoparticles. *Chem. Mater.* **2009**, *21*, 1524.
(8) Zhang, J. N.; Zhang, X. L.; Zhou, Y. C.; Guo, S. J.; Wang, K. X.; Liang, Z. Q.; et al. Nitrogen-Doped Hierarchical Porous Carbon Nanowhisker Ensembles on Carbon Nanofiber for High-Performance Supercapacitors. *ACS Sustainable Chem. Eng.* **2014**, *2* (6), 1525−1533.
(9) Kong, L. J.; Xiong, Y.; Sun, L. P.; Tian, S. H.; Xu, X. Y.; Xu, C. Y.; et al. Sorption performance and mechanism of a sludge-derived char as porous carbon-based hybrid adsorbent for benzene derivatives in aqueous solution. *J. Hazard. Mater.* **2014**, *274*, 205.
(10) Xue, C. F.; Tu, B.; Zhao, D. Y. Evaporation-Induced Coating and Self-Assembly of Ordered Mesoporous Carbon-Silica Composite Monoliths with Macroporous Architecture on Polyurethane Foams. *Adv. Funct. Mater.* **2008**, *18*, 3914.
(11) Deng, Y.; Liu, C.; Yu, T.; Liu, F.; Zhang, F.; Wan, Y.; Zhang, L.; Wang, C.; Tu, B.; Webley, P. A.; Wang, H.; Zhao, D. Facile Synthesis of Hierarchically Porous Carbons from Dual Colloidal Crystal/Block Copolymer Template Approach. *Chem. Mater.* **2007**, *19*, 3271.
(12) Wang, Z. Y.; Stein, A. Morphology Control of Carbon, Silica, and Carbon/Silica Nanocomposites: From 3D Ordered Macro-/Mesoporous Monoliths to Shaped Mesoporous Particles. *Chem. Mater.* **2008**, *20*, 1029.
(13) Estevez, L.; Dua, R.; Bhandari, N.; Ramanujapuram, A.; Wang, P.; Giannelis, E. P. A facile approach for the synthesis of monolithic hierarchical porous carbons − high performance materials for amine based CO_2 capture and supercapacitor electrode. *Energy Environ. Sci.* **2013**, *6*, 1785.
(14) Stein, A.; Wang, Z. Y.; Fierke, M. A. Functionalization of Porous Carbon Materials with Designed Pore Architecture. *Adv. Mater.* **2009**, *21*, 265.
(15) Wang, D. W.; Li, F.; Liu, M.; Lu, G. Q.; Cheng, H. M. 3D Aperiodic Hierarchical Porous Graphitic Carbon Material for High-Rate Electrochemical Capacitive Energy Storage. *Angew. Chem., Int. Ed.* **2008**, *47*, 373.
(16) Hu, Y. S.; Adelhelm, P.; Smarsly, B. M.; Hore, S.; Antonietti, M.; Maier, J. Synthesis of Hierarchically Porous Carbon Monoliths with Highly Ordered Microstructure and Their Application in Rechargeable Lithium Batteries with High-Rate Capability. *Adv. Funct. Mater.* **2007**, *17*, 1873.
(17) Xing, W.; Huang, C. C.; Zhuo, S. P.; Yuan, X.; Wang, G. Q.; Hulicova-Jurcakova, D.; et al. Hierarchical porous carbons with high performance for supercapacitor electrodes. *Carbon* **2009**, *47*, 1715.
(18) Liang, Y. R.; Wu, B. M.; Wu, D. C.; Xu, F.; Li, Z. H.; Luo, J. W.; Zhong, H.; Fu, R. W.; Matyjaszewski, K. Ultrahigh surface area hierarchical porous carbons based on natural well-defined macropores in sisal fibers. *J. Mater. Chem.* **2011**, *21*, 14424.
(19) Payne, E. K.; Rosi, N. L.; Xue, C.; Mirkin, C. A. Sacrificial Biological Templates for the Formation of Nanostructured Metallic Microshells. *Angew. Chem., Int. Ed.* **2005**, *44*, 5064.
(20) Chao, C.; Zhang, B.; Zhai, R.; Xiang, X.; Liu, J. D.; Chen, R. F. Natural Nanotube-Based Biomimetic Porous Microspheres for Significantly Enhanced Biomolecule Immobilization. *ACS Sustainable Chem. Eng.* **2014**, *2* (3), 396.
(21) Chiang, C.-Y.; Epstein, J.; Brown, A.; Munday, J. N.; Culver, J. N.; Ehrman, S. Biological Templates for Antireflective Current Collectors for Photoelectrochemical Cell Applications. *Nano Lett.* **2012**, *12*, 6005.
(22) Petkovich, N. D.; Stein, A. Controlling macro- and mesostructures with hierarchical porosity through combined hard and soft templating. *Chem. Soc. Rev.* **2013**, *42*, 3721.
(23) Liu, H. J.; Wang, X. M.; Cui, W. J.; Dou, Y. Q.; Zhao, D. Y.; Xia, Y. Y. Highly ordered mesoporous carbon nanofiber arrays from a crab shell biological template and its application in supercapacitors and fuel cells. *J. Mater. Chem.* **2010**, *20*, 4223.
(24) Davis, S. A.; Burkett, S. L.; Mendelson, N. H.; Mann, S. Bacterial templating of ordered macrostructures in silica and silica-surfactant mesophases. *Nature* **1997**, *385*, 420.
(25) Chung, S.-H.; Manthiram, A. Eggshell Membrane-Derived Polysulfide Absorbents for Highly Stable and Reversible Lithium−Sulfur Cells. *ACS Sustainable Chem. Eng.* **2014**, *2* (10), 2248.
(26) Rambo, C. R.; Sieber, H. Novel Synthetic Route to Biomorphic Al_2O_3 Ceramics. *Adv. Mater.* **2005**, *17*, 1088.
(27) Li, J. B.; Xu, Q.; Wang, J. G.; Jiao, J. X.; Zhang, Z. W. Controlled Synthesis of Monolithic Hierarchical Porous Materials Using Wood as a Template with Assistance of Supercritical Carbon Dioxide. *Ind. Eng. Chem. Res.* **2008**, *47*, 7680.
(28) Bantsis, G.; Betsiou, M.; Bourliva, A.; Yioultsis, T.; Sikalidis, C. Synthesis of porous iron oxide ceramics using Greek wooden templates and mill scale waste for EMI applications. *Ceram. Int.* **2012**, *38*, 721.
(29) Pan, J. M.; Cheng, X. N.; Yan, X. H.; Zhang, C. H. Preparation and hierarchical porous structure of biomorphic woodceramics from sugarcane bagasse. *J. Eur. Ceram. Soc.* **2013**, *33*, 575.
(30) Gong, Y. T.; Wang, H. Y.; Wei, Z. Z.; Xie, L.; Wang, Y. An Efficient Way To Introduce Hierarchical Structure into Biomass-Based Hydrothermal Carbonaceous Materials. *ACS Sustainable Chem. Eng.* **2014**, *2* (10), 2435−2441.
(31) Lu, Y.; Fan, H.; Stump, A.; Ward, T. L.; Rieker, T.; Brinker, C. J. Aerosol-assisted self-assembly of mesostructured spherical nanoparticles. *Nature* **1999**, *398*, 223.
(32) Liu, R. L.; Shi, Y. F.; Wan, Y.; Meng, Y.; Zhang, F. Q.; Gu, D.; Chen, Z. X.; Tu, B.; Zhao, D. Y. Triconstituent Co-assembly to Ordered Mesostructured Polymer−Silica and Carbon−Silica Nanocomposites and Large-Pore Mesoporous Carbons with High Surface Areas. *J. Am. Chem. Soc.* **2006**, *128*, 11652.
(33) Xia, L. Y.; Zhang, M. Q.; Rong, M. Z.; Guo, K. K.; Hu, Y. C.; Wu, Y. Q.; Czigany, T. An easy soft-template route to synthesis of wormhole-like mesoporous tungsten carbide/carbon composites. *Compos. Sci. Technol.* **2012**, *72*, 1651.

DOI: 10.1021/acssuschemeng.5b00243
ACS Sustainable Chem. Eng. 2015, 3, 1724−1731